



An improved seed-mediated growth method to coat complete silver shells onto silica spheres for surface-enhanced Raman scattering

Tao Liu^a, Dongsheng Li^{a,*}, Deren Yang^a, Minhua Jiang^b

^a State Key Laboratory of Silicon Materials, and Department of Materials Science and Engineering, Zhejiang University, Hangzhou 310027, People's Republic of China

^b State Key Laboratory of Crystal Growth, Shandong University, Jinan, People's Republic of China

ARTICLE INFO

Article history:

Received 8 May 2011

Received in revised form 21 June 2011

Accepted 10 July 2011

Available online 22 July 2011

Keywords:

Nanoparticle

Nanoshell

Silver

Surface plasmon

Surface-enhanced Raman scattering

ABSTRACT

We synthesized SiO₂@Ag core-shell particles with uniform and complete silver shells with an improved seed-mediated growth method. Silver nuclei produced on silica spheres with an electroless plating method served as nucleation sites for the growth of outer silver shells. By adjusting the Ag/SiO₂ ratio, the thickness of silver shells was tuned, and the extinction peaks of SiO₂@Ag particles shifted from visible to near-infrared (NIR) region. Comparing with previously reported methods, two important strategies were employed in the growth step of silver shells. First, polyvinylpyrrolidone (PVP) was added to control the isotropic growth of silver nuclei and improve the stability of core-shell particles. Second, the growth step of the outer silver shells was completed in a few seconds by increasing the reaction temperature and pH value. Furthermore, the SiO₂@Ag core-shell particles were self-assembled into a monolayer, which served as a good SERS substrate.

© 2011 Elsevier B.V. All rights reserved.

1. Introduction

Noble metal nanostructures have attracted much attention due to their fascinating surface plasmon properties [1,2], which are determined by the type, shape, size of the metals, and dielectric surrounding [3,4]. For solid noble metallic nanospheres, the plasmon resonance frequency is generally within the visible region. In order to tune the plasmon resonance frequency to near-infrared region (NIR), metallic nanostructures with special shapes such as Au or Ag nanorods [5], nano-plates [6], nanocubes [7], or hybrid structures such as core-shell particle [8] have been synthesized. Among the structures mentioned above, the plasmon resonance frequency of core-shell particles is much easily tuneable due to their composite structures. In general, the plasmon resonance peaks of core-shell particles depend on the size of the cores, the thickness of metal shells and the coupling between neighbouring particles [9]. Due to large tuneable scale of extinction peaks, Au or Ag shells and their assembly have been used in photoluminescence enhancement [10], biological sensing [11], photothermal therapy [12], photonic crystal [13], surface-enhanced Raman scattering (SERS) [14] and so on. For the above application, it is necessary to obtain mono-disperse core-shell particles with uniform and thickness-controllable metal shells.

Though uniform gold shells can be easily synthesized by the literature procedure [15], it is still not easy to control the morphology of SiO₂@Ag particles. Over the past years, there has been much effort on synthesizing SiO₂@Ag particles, including electroless plating [16–19], layer by layer (LBL) [20], thermal deposition [21], and so on. However, SiO₂@Ag particles with complete silver shells, good dispersion and controllable thickness are still difficult to obtain conveniently. In this paper, we synthesize mono-disperse SiO₂@Ag particles with uniform and complete silver shells with an improved seed-mediated electroless plating method. The isotropic growth of all the silver nuclei in a few seconds and the stabilization provided by polyvinylpyrrolidone (PVP) are essential to obtain complete silver shells. The thickness of silver shells was tuned by adjusting the Ag/SiO₂ ratio, which resulted in tuneable plasmon resonance frequency of the core-shell particles. Moreover, we prepared monolayer films composed of closely packed SiO₂@Ag particles conveniently through an oil-water interfacial self-assembly method. The monolayer exhibited high SERS effect due to high density of SiO₂@Ag particles and large amount of hot spots.

2. Experimental

2.1. Materials

Polyvinylpyrrolidone (PVP, k30), silver nitrate, formaldehyde (37%), tetraethoxysilane (TEOS), absolute ethanol, hexane, ammonia (28%) were supplied by Sino-pharm Chemical Reagent Co. Ltd. SnCl₂·2H₂O was obtained from Alpha company. Rhodamine 6G

* Corresponding author. Tel.: +86 0571 8795 2752; fax: +86 0571 8795 2322.
E-mail address: mselds@zju.edu.cn (D. Li).

(R6G) was obtained from Sigma–Aldrich Company. Home-made Milli-Q water was used.

2.2. Preparation of $\text{SiO}_2\text{@Ag}$ core-shell particles

In a typical synthetic process, silica microspheres with diameter of 300 nm prepared by the Stöber method [22] were mixed with 3% $\text{SnCl}_2 \cdot 2\text{H}_2\text{O}$ aqueous solution (containing small amount of hydrochloric acid to avoid hydrolyzation of SnCl_2) for 30 min, then the mixture was centrifuged to remove unabsorbed Sn^{2+} and re-dispersed in water. The Sn^{2+} functioned silica colloids were added into 0.35 mol L^{-1} ammonia silver nitrate solution under ultrasonic wave. The reaction lasted for 20 min, resulting in silver nuclei decorated silica spheres. Different amount of rinsed silver nuclei decorated silica sphere solution was dispersed in 0.25 mmol L^{-1} silver nitrate aqueous solution containing 0.25 wt% (11 mM L^{-1} in term of PVP monomer) PVP, then excessive amount of 37% formaldehyde and 28% ammonia were added in sequence. The $\text{SiO}_2\text{@Ag}$ core-shell particles were obtained in a few seconds. The whole reaction was carried at 30°C .

2.3. Preparation of a monolayer of $\text{SiO}_2\text{@Ag}$ particles

The $\text{SiO}_2\text{@Ag}$ particles were collected by centrifugation and re-dispersed in water. Then 10 mL $\text{SiO}_2\text{@Ag}$ particle aqueous solution was poured into a glass container, and 5 mL hexane was added to create a clear hexane–water interface. 1–2 mL ethanol was dropped to the liquid slowly, then $\text{SiO}_2\text{@Ag}$ particles were assembled at the hexane–water interface, and a film formed within a few minutes.

2.4. Preparation of SERS substrates

Clean silicon wafers were dipped into the solution in Section 2.3 with a small inclination angle, and lifted carefully. Then the $\text{SiO}_2\text{@Ag}$ monolayer was transferred onto silicon substrates, and dried in an oven. 25 μL R6G ethanol solution with different concentration (10^{-1} – $10^{-7} \text{ mol L}^{-1}$) was dropped onto $\text{SiO}_2\text{@Ag}$ particle film covered silicon wafers and bare silicon wafers (as reference).

2.5. Characterization

The morphology of $\text{SiO}_2\text{@Ag}$ particles was characterized by transmission electron microscope (TEM, CM200; Philips), High resolution TEM (HRTEM, JEM 2010) and scanning electron microscope (SEM, S-4800; Hitachi). The extinction property test of particle colloids was carried on UV–vis spectrophotometer (UV-3150; Shimadzu). The obtained samples were characterized by X-ray powder diffraction (XRD) using an X'Pert PRO X-ray diffractometer with the graphite monochromatized $\text{Cu K}\alpha$ radiation. The SERS spectra test were performed under object lens of an Olympus microscopy with the 514.5 nm laser and a PIXIS: 100BR charge-coupled device (CCD) detector connected to Acton SpectraPro-2500i.

3. 3 Result and discussion

3.1. Characterization of $\text{SiO}_2\text{@Ag}$ core-shell particles

It is well known that the seed-mediated growth method is a versatile method to grow metal particles by adding new atoms onto the

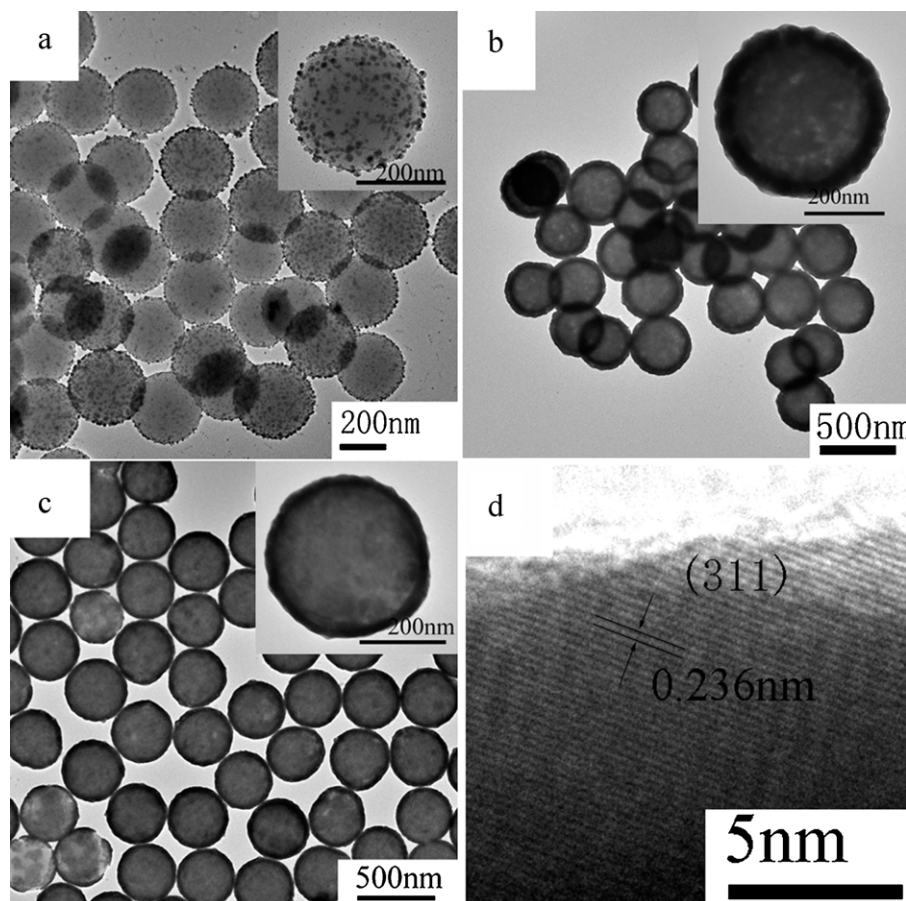


Fig. 1. TEM images of products: (a) silver nuclei decorated silica spheres; (b and c) $\text{SiO}_2\text{@Ag}$ core-shell particles with (b) 50 nm and (c) 20 nm thick shell; (d) HRTEM picture of a part of a silver shell in (b).

existing nuclei. Few new nuclei form in the growth process due to the low concentration of reactant, which is beneficial for synthesis of particles with narrow size distribution. Here the seed-mediated method is used to grow uniform silver shells on silica spheres. The silver nuclei decorated silica spheres were obtained through an electroless plating process similar with the method developed by Liz-Marzan and co-workers [16] and Wang and co-workers [23]. Firstly, a layer of Sn^{2+} was absorbed onto negatively charged silica surface by electrostatic attraction. Then Ag^+ was reduced by Sn^{2+} immediately and deposited onto the silica spheres directly. The morphology of the silver nuclei decorated silica microspheres is shown in Fig. 1a, and a high magnification image is shown as an inset. Dense and uniform silver nuclei with the size of about 5 nm covered the silica surface, and few free silver particles were observed. After ammonia was added, Ag^+ was reduced by formaldehyde in a few seconds. And the Ag atoms produced deposited on the silver nuclei on the surface of silica spheres, resulting in complete silver shells surrounding the silica spheres, as shown in Fig. 1b and c. From the photos, we can see the silver shells are complete and uniform, without obvious aggregation and free silver particles. The thickness of silver shells shown in Fig. 1b and c is about 50 nm and 20 nm, respectively. The thickness is tuned by changing the Ag/ SiO_2 ratio in the growth process of silver shells. With the increase of the amount of silica sphere solution, the thickness of silver shells is decreased. A HRTEM image of a part of a silver shell in Fig. 1b is shown in Fig. 1d, which shows that the space between two crystal planes is 0.236 nm, corresponding to the (1 1 1) plane of silver with fcc phase.

The SEM images of silver shells are shown in Fig. 2. The SEM image of the SiO_2 @Ag particles with 50 nm shells in Fig. 2a shows

that the whole size of the hybrid particles is rather uniform. The thickness of silver shells can be roughly determined by measuring the thickness of hollow silver shells, which were obtained by dissolving the silica cores with diluted HF solution. The SEM pictures of 50 nm, 30 nm and 20 nm hollow silver shells are shown in Fig. 2b–d, respectively, and a high magnification image of each is shown in the insets. Thick hollow shells retain sphere shape well, which suggests that the silver shells were complete and stable. The hollow silver shells were potentially used as active catalysis [24].

The XRD pattern of SiO_2 @Ag particles is shown in Fig. 3. Four diffraction peaks (2 θ) at 38.1°, 44.2°, 64.4° and 77.4° correspond to (1 1 1), (2 0 0), (2 2 0) and (3 1 1) planes of silver with face-centered-cubic (fcc) phase, respectively. Therefore, the shells are composed of pure silver, and no silver oxide was detected.

3.2. Growth mechanism

Generally, the formation of silver shells is a seed-mediated process. The existence of uniform silver nuclei is necessary under our experiment condition. We did control experiments using silica spheres without Ag seeds. At 30 °C, the reaction was very slow and the colour of the solution did not change in 1 h, which suggested that the growth of existing Ag seed was much easier than the formation of new silver particles. When the reaction temperature was raised to 45 °C, the reaction became faster, and the colour of the solution changed within 10 min. The SEM image of the sample is shown in Fig. 4, from which it can be seen that silver particles did not deposit on the surface of silica spheres. Flores et al. showed that in the presence of ammonia, direct reaction between silanols and silver–ammonia complexes yielded the complete coating of silica

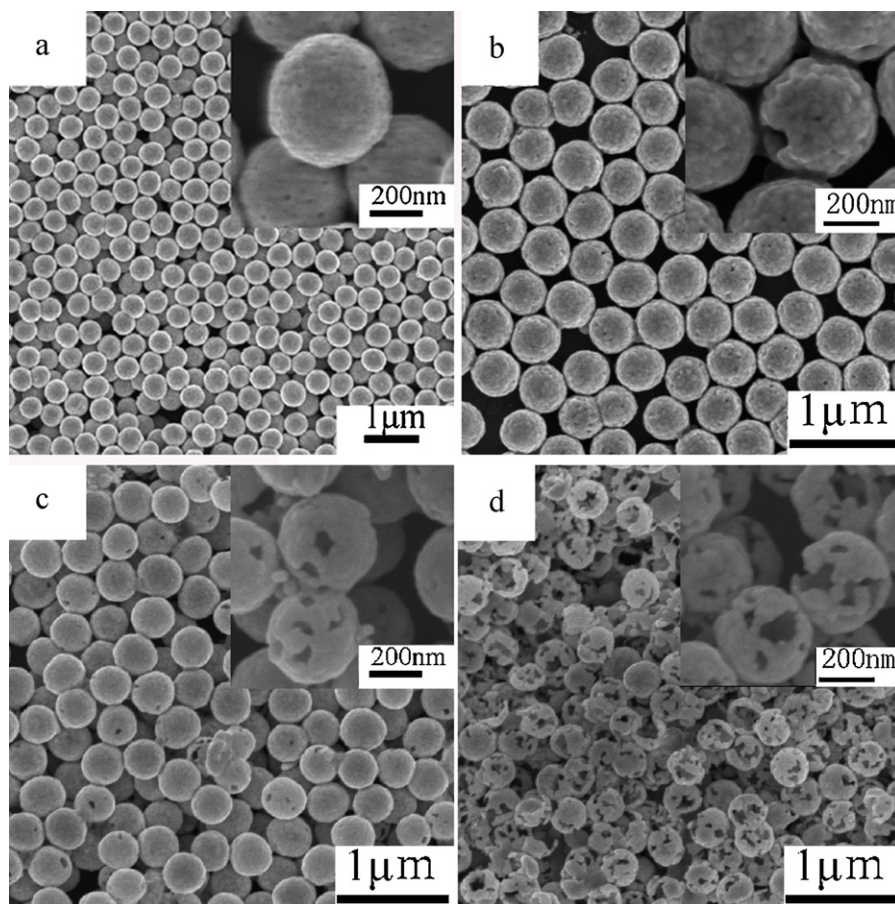


Fig. 2. SEM images of products: (a) SiO_2 @Ag particles with 50 nm thick shells; (b–d) silver hollow shells with thickness of (b) 50 nm, (c) 30 nm and (d) 20 nm. The insets are images taken at higher magnification of the same products.

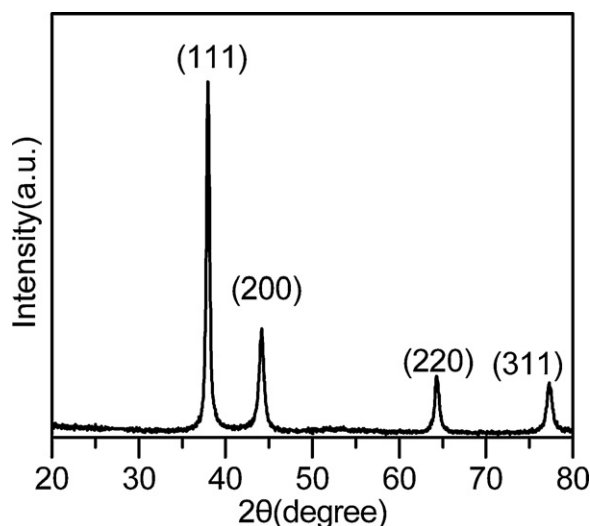


Fig. 3. The XRD spectrum of SiO₂@Ag particles.

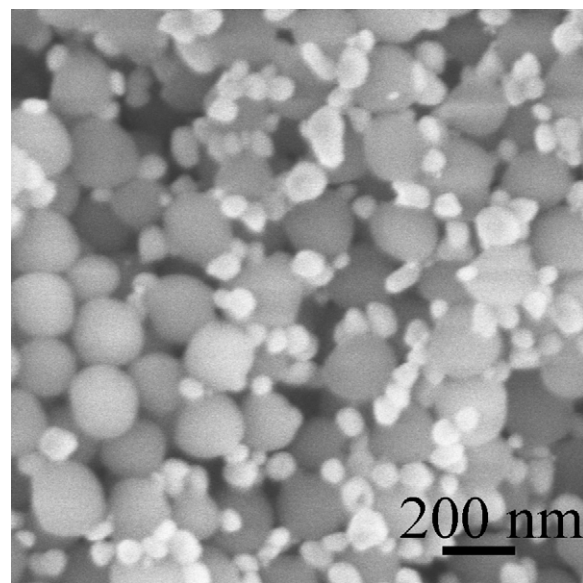


Fig. 5. The SEM image of the sample prepared with SiO₂ spheres without Ag seed.

spheres by a nanometric smooth silver layer [18]. However, as the amount of the ammonia here was not as high as that in the method of Flores, the direct reaction between silanols and silver-ammonia complexes did not take place.

To investigate the influence of reaction rate of the shell-forming process on the coating results, we carried out control experiments under different conditions. It is considered that the reduction ability of CH₂O was influenced greatly by temperature (T) and pH value [25]. In our experiment, before ammonia was added, no silver particles formed due to low pH value of the mixture, and once the ammonia solution was added, the colour of the mixture changed in a few seconds, suggesting the formation of silver particles. If lowering the reaction temperature, the reaction rate was reduced obviously. In fact, the colour change became very slow when the reaction was carried at 10 °C, and large separated silver particles formed on the silica surface, as shown in Fig. 5a. In general, at relative higher temperature and higher pH value, all the silver nuclei can grow up fast at the same time. Otherwise, at low temperature, a part of nuclei whose size is larger than critical value (determined by thermodynamics) grow first. In this condition, silver atoms are consumed by large silver particles only. Then Ostwald ripening among silver particles of different sizes in the later growth process results in separated particles on the silica spheres, and complete silver shells cannot be obtained [26]. Rapid reaction in growth step is rarely used in common seed-mediated process, but it is very important in our strategy, as the morphology of silver shells is determined by the kinetic factor.

PVP was commonly used as a surfactant in preparation of silver nanoparticles due to its good affinity to silver surface and good solubility in many solvents [27]. But in former strategies for the preparation of SiO₂@Ag particles, polymer surfactants were rarely used. Here PVP was used to avoid aggregation of core-shell particles and to control the growth of silver shells. The role of PVP in controlling the shape of silver particles is related with the molar ratio between PVP and AgNO₃ [27]. In our experiments, the molar ratio between PVP and AgNO₃ was relatively high (>10), and PVP wholly covered all the facets of silver particles, which facilitated isotropic growth of silver particles, and this contributed much to the formation of smooth silver shells. On the other hand, PVP avoided the aggregation of particles via steric effects [28]. The core-shell particles obtained can disperse well in water. From our observation, if PVP was not added, the particles easily aggregated. However, it was found that the concentration of PVP was required to be within

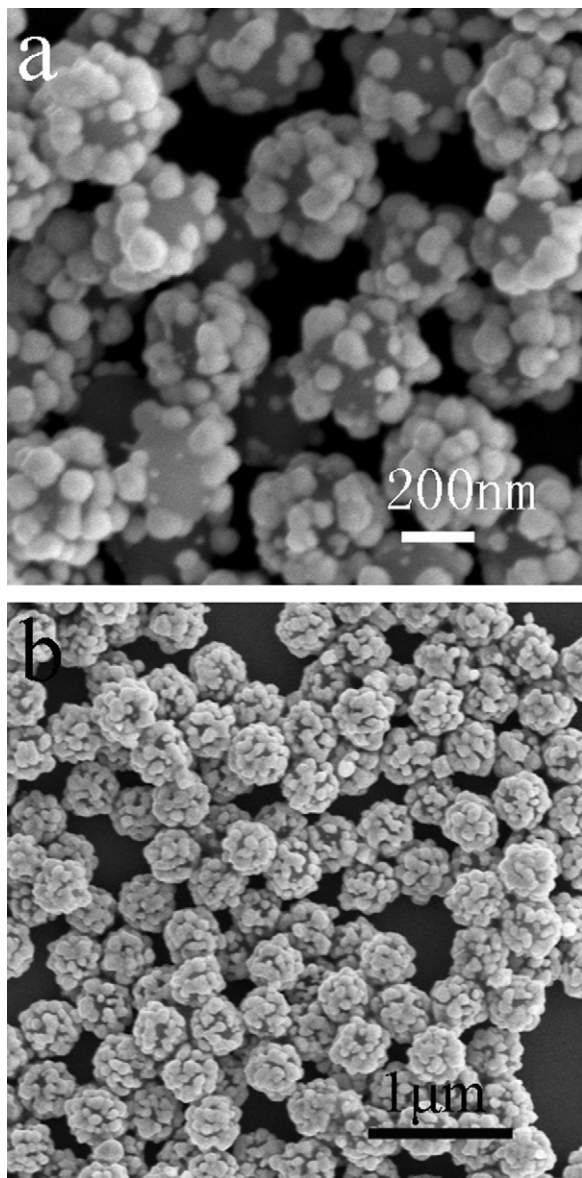


Fig. 4. The SiO₂@Ag particles prepared at (a) 10 °C and (b) with 0.5% PVP.

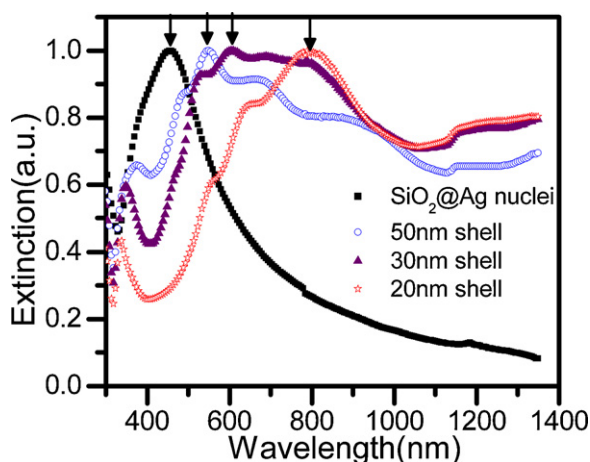


Fig. 6. Normalized extinction spectra of silver nuclei decorated silica microspheres and $\text{SiO}_2\text{@Ag}$ core-shell particles in aqueous solution.

an appropriate region, as PVP could reduce the reduction rate of Ag^+ . When 0.5 wt% PVP was used, the colour change of the mixture became much slower. Silver atoms deposit onto silica spheres in the form of large particles, as shown in Fig. 5b. This is in accordance with our discussion in last paragraph.

3.3. The extinction property of core-shell particles

The extinction property of dielectric-metal core-shell particles has been paid much attention because of its large tunability due to the coupling between inner and outer surface of metal shells [9]. Similar with $\text{SiO}_2\text{@Au}$ core-shell structures, $\text{SiO}_2\text{@Ag}$ particles we obtained showed different extinction property comparing with silver particles. The extinction spectra of silver nuclei decorated silica microspheres and $\text{SiO}_2\text{@Ag}$ particles are shown in Fig. 6. For the silver nuclei, the extinction peak is at 420 nm, while that of the core-shell particles spreads from visible to NIR region. Furthermore, with the decrease of silver shell thickness, the extinction peaks shift to long wavelength region gradually. For 50 nm shells, the main extinction peak (shown by the arrow) locates at about 500 nm, while the extinction peak of 20 nm shells is tuned to 800 nm. The large red-shift is attributed to stronger coupling of the inner and outer surfaces of silver shell. The $\text{SiO}_2\text{@Ag}$ particles with extinction peaks at NIR region are very useful in biological and medical application as human tissues are transparent in NIR region. Besides, as the particle size is beyond the dipole limit, multipolar

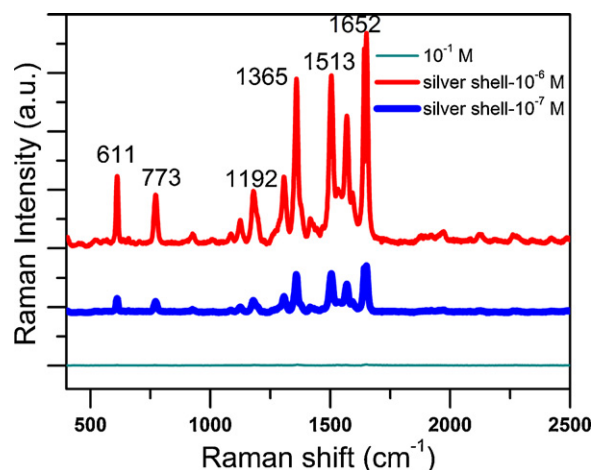


Fig. 8. Raman scattering spectra of different concentration of R6G on $\text{SiO}_2\text{@Ag}$ particle films and on a bare silicon substrate.

plasmon resonance of the silver shells results in the appearance of several shoulders in each spectrum [15].

3.4. Application of $\text{SiO}_2\text{@Ag}$ particles in SERS

It would be meaningful to explore whether $\text{SiO}_2\text{@Ag}$ particles can be used as SERS substrates. Though $\text{SiO}_2\text{@Ag}$ films prepared by evaporating particle solution on substrates have showed very high SERS effect [14], the enhancement factor of SERS would vary in different spots, as the film is non-uniform due to the uncontrollable evaporating process. Here, a uniform film composed of closely packed $\text{SiO}_2\text{@Ag}$ particles with 30 nm shell was prepared through an oil–water interfacial assembly method, which has been used to assemble Au particles, Au nanorods and PVP stabilized Pt particles [29,30].

From the optical image of the film in a glass container in Fig. 7a, it can be seen the whole film displays a mirror-like colour by virtue of its high reflection efficiency. The area of the film can be as large as several square centimetres. Further analysis of the film can be obtained from the SEM image of $\text{SiO}_2\text{@Ag}$ monolayer on silicon wafer in Fig. 7b. It can be seen that the film composed of closely packed $\text{SiO}_2\text{@Ag}$ particles is uniform over the whole SEM picture. The space between particles caused by PVP coating is below 10 nm, which would leads to extremely large amounts of hot spots in the inter-particles regions. At these hot spots, the SERS enhancement

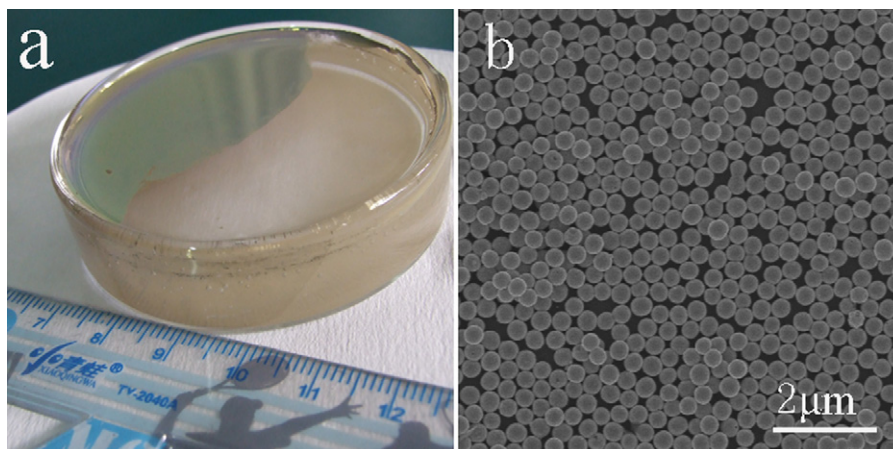


Fig. 7. (a) photo image of a $\text{SiO}_2\text{@Ag}$ film; (b) SEM picture of a part of a $\text{SiO}_2\text{@Ag}$ film on a silicon substrate.

is much higher [30]. For example, layers composed of close-packed Au nanorods display high SERS activity [31].

The SERS activity of the SiO₂@Ag film was tested by R6G dye, which is widely used as the SERS Probe. The Raman scattering results are shown in Fig. 8. Several peaks during 500–2000 cm⁻¹ are typical Raman peaks of R6G. The Raman scattering intensity increases with the concentration of R6G molecule. Comparing with reference sample, the Raman intensity of R6G is so greatly enhanced that the Raman peaks of R6G with 10⁻⁷ M solution are still very strong.

4. Conclusion

In conclusion, we synthesized complete and smooth silver shells on silica microspheres using an improved seed-mediated growth method. By adjusting the Ag/SiO₂ ratio, the thickness of the silver shells was tuned, which resulted in tuneable plasmon peaks. PVP acts as a good stabilizer during the growth step. Rapid reaction is necessary to obtain smooth shells. The morphology of the silver shells can also be tuned by changing the PVP concentration. Uniform films of SiO₂@Ag particles were fabricated through a hexane-water interfacial self-assembly process, and the films acted as efficient SERS substrates due to high density of SiO₂@Ag particles and hot spots. SiO₂@Ag particles we prepared are supposed to be used in PL enhancement and plasmonic solar cells. Our strategy for coating silver onto silica microspheres may be used to deposit silver onto other templates.

Acknowledgements

The authors express their appreciation to the Fundamental Research Funds for the Central Universities (Program No. 2010QNA4001) and 863 program (No. 2011AA050517) for the financial support.

References

- [1] W.A. Murray, W.L. Barnes, Plasmonic materials, *Adv. Mater.* 19 (2007) 3771–3782.
- [2] M.A. Noginov, G. Zhu, A.M. Belgrave, R. Bakker, V.M. Shalae, E.E. Narimanov, S. Stout, E. Herz, T. Suteewong, U. Wiesner, Demonstration of a spaser-based nanolaser, *Nature* 460 (2009) 1110–1113.
- [3] Y. Xia, Y.J. Xiong, B. Lim, S.E. Skrabalak, Shape-controlled synthesis of metal nanocrystals: simple chemistry meets complex physics, *Angew. Chem. Int. Ed.* 48 (2009) 60–103.
- [4] T. Liu, D.S. Li, Y. Zou, D.R. Yang, H.L. Li, Y.M. Wu, M.H. Jiang, Preparation of metal@silica core-shell particle films by interfacial self-assembly, *J. Colloid Interface Sci.* 350 (2010) 58–62.
- [5] B. Nikoobakht, M.A. El-Sayed, Preparation and growth mechanism of gold nanorods (NRs) using seed-mediated growth method, *Chem. Mater.* 15 (2003) 1957–1962.
- [6] S.H. Chen, D.L. Carroll, Silver nanoplates: size control in two dimensions and formation mechanisms, *J. Phys. Chem.* 108 (2004) 5500–5506.
- [7] D.B. Yu, V.W.W. Yam, Controlled synthesis of monodisperse silver nanocubes in water, *J. Am. Chem. Soc.* 126 (2004) 13200–13201.
- [8] N. Halas, Playing with plasmons. Tuning the optical resonant properties of metallic nanoshells, *Mater. Res. Bull.* 30 (2005) 362–367.
- [9] E. Prodan, C. Radloff, N.J. Halas, P. Nordlander, A hybridization model for the plasmon response of complex nanostructures, *Science* 302 (2003) 419–422.
- [10] F. Tam, G.P. Goodrich, B.R. Johnson, N.J. Halas, Plasmonic enhancement of molecular fluorescence, *Nano Lett.* 7 (2007) 496–501.
- [11] G. Raschke, S. Brogl, A.S. Susha, A.L. Rogach, T.A. Klar, J. Feldmann, B. Fieres, N. Petkov, T. Bein, A. Nichtl, K. Kurzinger, Gold nanoshells improve single nanoparticle molecular sensors, *Nano Lett.* 4 (2004) 1853–1857.
- [12] A.M. Gobin, M.H. Lee, N.J. Halas, W.D. James, R.A. Drezek, J.L. West, Near-infrared resonant nanoshells for combined optical imaging and photothermal cancer therapy, *Nano Lett.* 7 (2007) 1929–1934.
- [13] J.H. Zhang, J.B. Liu, S.Z. Wang, P. Zhan, Z.L. Wang, N.B. Ming, Facile methods to coat polystyrene and silica colloids with metal, *Adv. Funct. Mater.* 14 (2004) 1089–1096.
- [14] J.B. Jackson, N.J. Halas, Surface-enhanced Raman scattering on tunable plasmonic nanoparticle substrates, *Proc. Natl. Acad. Sci. USA* 101 (2004), 17930–17935.
- [15] S.J. Oldenburg, J.B. Jackson, S.L. Westcott, N.J. Halas, Infrared extinction properties of gold nanoshells, *Appl. Phys. Lett.* 75 (1999) 2897–2899.
- [16] Y. Kobayashi, V. Salgueirino-Maceira, L.M. Liz-Marzan, Deposition of silver nanoparticles on silica spheres by pretreatment steps in electroless plating, *Chem. Mater.* 13 (2001) 1630–1633.
- [17] J.B. Jackson, N.J. Halas, Silver nanoshells: variations in morphologies and optical properties, *J. Phys. Chem. B* 105 (2001) 2743–2746.
- [18] J.C. Flores, V. Torres, M. Popa, D. Crespo, J.M. Calderón-Moreno, Deposition of silver nanoshell and reactivity of silver nanoparticles with surface silanols of submicrospherical silica, *J. Nanosci. Nanotechnol.* 9 (2009) 3177–3180.
- [19] J.C. Flores, V. Torres, M. Popa, D. Crespo, J.M. Calderón-Moreno, Variations in morphologies of silver nanoshells on silica spheres, *Colloids Surf. A: Physicochem. Eng. Aspects* 330 (2008) 86–90.
- [20] Z.J. Jiang, C.Y. Liu, Y. Liu, Z.Y. Zhang, Y.J. Li, Fabrication of silver nanoshell on functionalized silica sphere through layer-by-layer technique, *Chem. Lett.* 32 (2003) 668–669.
- [21] S.J. Park, T.V. Duncan, B.L. Sanchez-Gaytan, S.J. Park, Bifunctional nanostructures composed of fluorescent core and metal shell subdomains with controllable geometry, *J. Phys. Chem. C* 112 (2008) 11205–11210.
- [22] W. Stober, A. Fink, E. Bohn, Controlled growth of monodisperse silica spheres in micron size range, *J. Colloid Interface Sci.* 26 (1968) 62–69.
- [23] M.W. Zhu, G.D. Qian, Z.L. Hong, Z.Y. Wang, X.P. Fan, M.Q. Wang, Preparation and characterization of silica-silver core-shell structural submicrometer spheres, *J. Phys. Chem. Solids* 66 (2005) 748–752.
- [24] Z.L. Liu, B. Zhao, C.L. Guo, Y.J. Sun, F.G. Xu, H.B. Yang, Z. Li, Novel hybrid electrocatalyst with enhanced performance in alkaline media: hollow Au/Pd core/shell nanostructures with a raspberry surface, *J. Phys. Chem. C* 113 (2009) 16766–16771.
- [25] K.S. Chou, C.Y. Ren, Synthesis of nanosized silver particles by chemical reduction method, *Mater. Chem. Phys.* 64 (2000) 241–246.
- [26] X.W. Lou, C.L. Yuan, E. Rhoades, Q. Zhang, L.A. Archer, Encapsulation and Ostwald ripening of Au and Au-Cl complex nanostructures in silica shells, *Adv. Funct. Mater.* 16 (2006) 1679–1684.
- [27] B. Wiley, Y.G. Sun, B. Mayers, Y.N. Xia, Shape-controlled synthesis of metal nanostructures: the case of silver, *Chem. Eur. J.* 11 (2005) 454–463.
- [28] H.S. Wang, X.L. Qiao, J.G. Chen, X.J. Wang, S.Y. Ding, Mechanisms of PVP in the preparation of silver nanoparticles, *Mater. Chem. Phys.* 94 (2005) 449–453.
- [29] Y.J. Li, W.I.J. Huang, S.G. Sun, A universal approach for the self-assembly of hydrophilic nanoparticles into ordered monolayer films at a toluene/water interface, *Angew. Chem. Int. Ed.* 45 (2006) 2537–2539.
- [30] R.C. Maher, S.A. Maier, L.F. Cohen, L. Koh, A. Laromaine, J.A.G. Dick, M.M. Stevens, Exploiting SERS hot spots for disease-specific enzyme detection, *J. Phys. Chem. C* 114 (2010) 7231–7235.
- [31] S. Yun, M.K. Oh, S.K. Kim, S. Park, Linker-molecule-free gold nanorod films: effect of nanorod size on surface enhanced Raman scattering, *J. Phys. Chem. C* 113 (2009) 13551–13557.